Effect of Mixing on the Pore Structure of Alumina Extrudates

John Landers*, Mukundan Devadas*, **, Alexander V. Neimark*, Hye-Kyung Timken*, Adeola Ojo***, Arthur W. Chester***

(Received: 17 September 2009; accepted: 27 August 2010; published online: 10 December 2010)

DOI: 10.1002/ppsc.200900093

Abstract

The mixing conditions have a direct impact on the pore structure of alumina extrudates. We study the pore structure of samples prepared with two mixers: a standard Eirich mixer and a smaller yet more severe Fukae mixer, which operates at 1500 rpm. We present the development of a bimodal pore size distribution within the range of 25–150 Å produced by using the Fukae mixer. The pore structure consists of larger pores that grow at the expense of the smaller ones and can be tuned as a function of mixing time.

Keywords: alumina, bimodal, extrudate, mixing, pore size distribution

1 Introduction

Interest in the structural modification of mesoporous materials has garnered a tremendous amount of attention in recent years for its applications in catalysis, sorption and separation processes [1–6]. The ideal qualities of such materials include large surface areas for deposition, durability, and fast diffusion times for rapid molecular transport. However, the materials possessing high surface areas produced on a large scale generally lack the larger mesopores required for short diffusion times. It is therefore imperative in fields such as catalysis to provide for both large pores as pathways for swift diffusion as well as smaller ones to serve as active sites [7–9]. It is especially important in the petrochemical and petroleum industries where reactions typically occur with metals supported on porous metal oxides, the morphology of which affects the catalytic activity and product selectivity of the catalyst. However, the source material typically chosen for catalyst supports typically represents a powder which should be compacted into mechanically robust pellets [10–12]. This is accomplished by mixing the powder with a liquid binder in a process known as granulation. During this process a paste with sufficient plasticity is formed which adequate for extrusion; in some cases a minimal amount of acid (peptization) is required [11]. The advantage of extrusion is that it allows for the formation of pellets or spheres with a highly uniform cross-section [13–15]. These two processes that ultimately determine the interplay between porosity and the susceptibility of an extrudate to fracture, properties that tend to be orthogonal to each other. The former of these two properties will determine the amount of catalyst that can be loaded and its corresponding efficiency. As a result, generating pores that maximize the loading capabilities without sacrificing the extrudate strength and reactant transport serves as a major goal in catalyst preparation.

One such metal oxide that has long been utilized as a support is alumina [16, 17]. The predominance of its use is owed to its low relative cost, long stability, and its tunable surface area and porosity [18]. The latter of these enables it to be used in a broad range of applications as previously mentioned [19, 20]. By knowing which experimental parameters determine porosity, one can tailor porosity during manufacture and match it to a speci-

* J. Landers, Dr. M. Devadas, Prof. A.V. Neimark (corresponding author), Dr. A. Chester, Department of Chemical and Biochemical Engineering, Rutgers University, 98 Brett Road, Piscataway, New Jersey – 08854 (USA).
E-mail: aneimark@rutgers.edu

** Dr. M. Devadas, Institute of Chemical and Engineering Sciences, 1 Pesek Road, Jurong Island, 627833 (Singapore).

*** Dr. H Timken, Dr. A. Ojo, Chevron Energy Technology Company, Catalyst Department, Richmond, California – 94802 (USA).

fic need, thus improving efficiency. To date, however, any effort to manipulate a distribution to include a bimodal mesoporous distribution is accomplished by either a synthetic route [5, 20 – 25] , or the mixing of different phases of alumina consisting of various crystallite sizes. The former of these typically includes a template model using surfactants [5, 20, 21, 23 – 25], ionic liquids [22], and in some cases microemulsions [7]. In lieu of these approaches, we present a simple method for producing a bimodal mesoporous alumina support via high shear mixer (granulator). It was revealed that with granulation time there emerges a bimodal distribution in the mesoporous range that can be controlled simply by time.

2 Experimental

2.1 Materials

CATAPAL® B boehmite (Sasol) was used as alumina (AlOOH) source in the catalyst preparation. Distilled water was used as the wetting agent. 1M HNO_3 was purchased from Sigma Aldrich and was used as the peptizing agent.

2.2 Granulation and Extrusion

A laboratory high shear mixer (granulator) was used in the preparation of the catalyst. A high-shear granulator (Fukae Powtec) was used to granulate the alumina. It has an impeller, which is attached to the bottom of the vessel and a chopper, which is attached at the side of the vessel. Both, the impeller and chopper rotate in clockwise direction. The total capacity of the mixing vessel, is about 200 ~ 500 g of solids in each experimental batch. The reaction temperature was recorded from the thermocouple which is installed in the mixer along the periphery, so the indicated temperature may not be a quantitative characterization of the whole mass, but it does act as a qualitative indicator. Granulation was done by mixing alumina with the addition of distilled water (wetting agent). The mixture ratio was 45 : 55 (solid : water). Before adding the distilled water, alumina was mixed by keeping the impeller speed ~ 100 rpm and chopper speed ~ 500 rpm. This is done in order to deagglomerate the alumina. After a few minutes, when homogeneity in the mixture is obtained, the wetting agent is added with the help of a burette in order to have a more constant flow rate (0.0039 m^3/h). During the addition of distilled water the impeller and chopper speed is not increased. After the addition of all the water the rotation rate was increased to 500 rpm for the impeller and 1500 rpm for the chopper. Samples were then taken at 10 minutes intervals for extrusion and for characterization. The granulated sample is then extruded using a press (Carver, Inc.) and die whereby about 2 grams of sample was used and extruded through a 1/16” circular nozzle located at the base of the die.

2.3 Characterization

Nitrogen porosimetry analysis was measured using an AUTOSORB-1 series analyzer (Quantachrome). The resultant pore size distributions were calculated from the desorption isotherms using the Non-Local Density Functional Theory (NLDFT) [26, 27]. Prior to the analysis, the samples were calcined at 500 °C and degassed at 300 °C for 3 hrs. Particle size analysis was carried out in a LS-230 laser diffraction particle size analyzer (Beckmann-Coulter GmbH). Trace amounts of the sample was placed in a cell filled with distilled water and sonicated at an amplitude of 14 until the polarization intensity differential scattering reached a range between 45 and 55 %. The measurements were then allowed to run. Scattering of the light is converted to particle size using the Mie theory and a particle size distribution based on an alumina model. Crush strength measurements were measured using a DR. SCHLEUNIGER® model-6D tablet friability tester (Dr. Schleuniger Pharmatron AG). Between 25–50 extrudates were prepared of the same diameter and similar length to be crushed. Each sample was placed in the tester and two blocks applied a force until the sample fractured at which time a force in Newtons was registered.

3 Results and Discussion

3.1 Extrudate Characterization

Surface area and pore volume serve as an indicator to the loading capabilities of a support. Figure 1 shows the BET surface area while Figure 2 displays the total pore volume of the extruded samples. With increasing granulation time, there is considerable increase in the BET surface area and in the total pore volume. This increase starts to become less pronounced towards the end of the mixing time. By the addition of acid there is a considerable increase in the total pore volume over the entire mixing time. When calcined, the water is removed from the system, hence allowing adjacent particles to fuse together perhaps *via* neck formation. This allows for an increase in porosity and therefore an increase in surface area. With increasing acid concentration there was a decrease in surface area as well as a decrease in the total

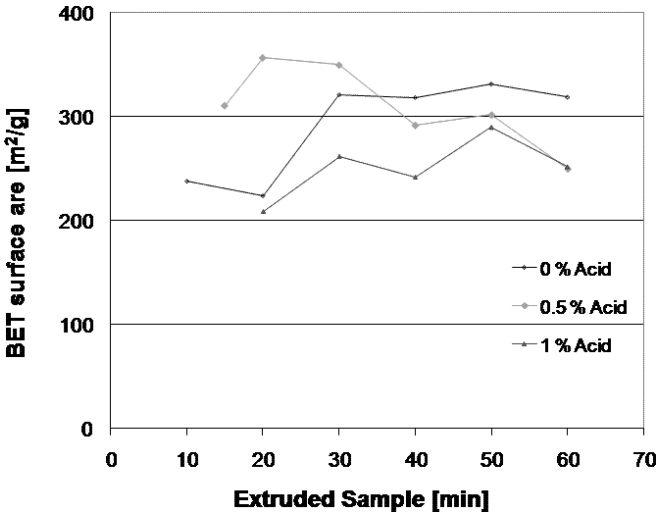

Fig. 1: BET surface areas results for the extruded samples as a function of mixing time.

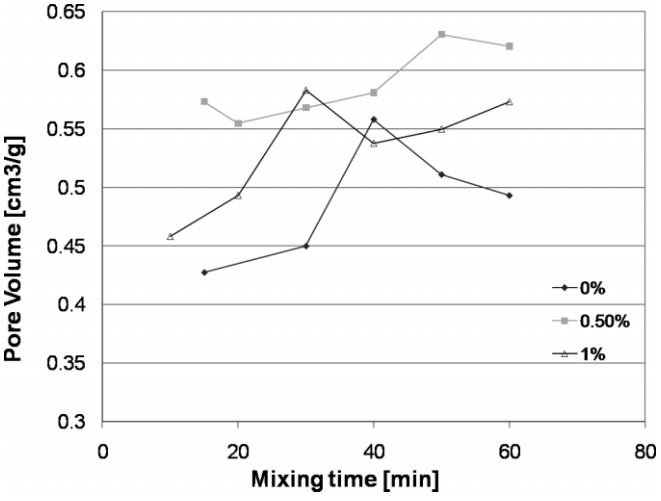

Fig. 2: Total pore volume results for the extruded samples as a function of mixing time.

pore volume. This is attributed to an increase in concentration of aluminum soluble species that fill the interstices between the particles [28]. Upon calcination of the extrudates from wet pellets, there is considerable amount of shrinkage taking place; thereby an increase in the strength of interparticle bonds is observed [29].

The NLDFT method [26, 27] was employed for the calculation of the pore size distribution. This method is preferred to the traditional Barrett-Joyner-Halenda (BJH) model for pore size analysis which progressively becomes inaccurate for pores smaller than 100 nm [26]. The calculated pore size distributions are presented in Figures 3 and 4. The pore size distributions are bimodal that is clearly dependent on mixing time. Initially, the distribution is dominated by one peak. As granulation time increases, the resultant extrudates reveal a second peak at a higher pore size. The emergence of this second peak evolves over the course of mixing whereby the first peak slowly dissipates at the expense of second one. Furthermore, the addition of acid imparts three effects. Firstly, there is a shift to higher pore sizes for both, the initial peak and the secondary peak. Secondly, the emergence of the secondary peak occurs more rapidly and surpasses the first in height in less time. Lastly, the more peptized systems show a height increase for both peaks at all stages of mixing.

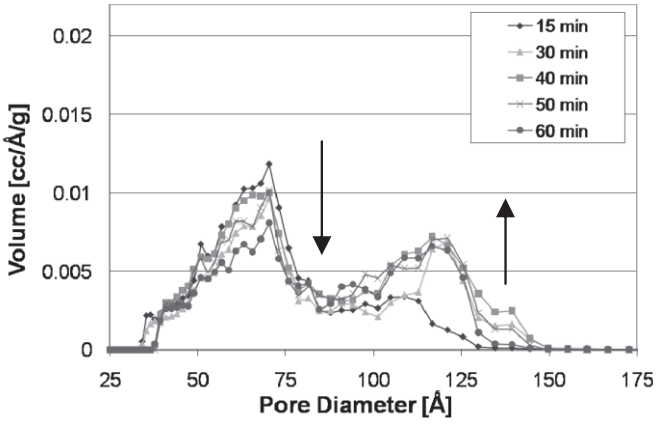

Fig. 3: Pore size distribution as a function of mixing time for 0 % acid .

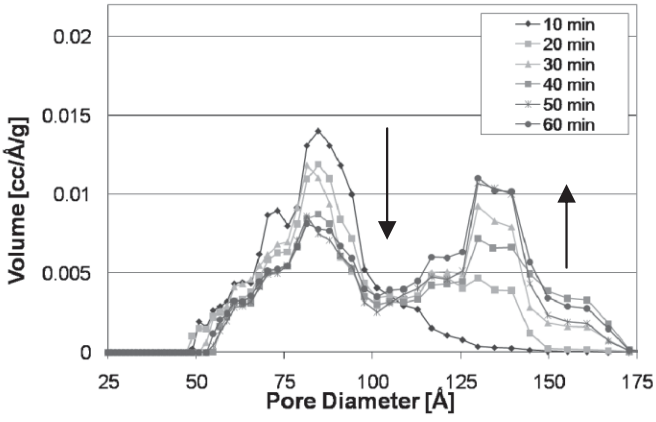

Fig. 4: Pore size distribution as a function of mixing time for 1 % acid.

The failure of catalyst strength in a fixed bed converter causes maldistribution of fluid flow. This in turn can lead to a large pressure drop through the bed which can result in a low efficiency of catalysis and in extreme cases plant shut down. The typical culprit for strength failure in these catalysts are brittle fractures [30]. For porous catalysts containing defects, dislocations and discontinuations, the expending of the micro cracks under tensile stress concentrated around the edges of flaws is the primary reason for fracture [31]. It is thus necessary

to have extrudates that are both porous for adsorption as well as durable. Crush strength measurements were taken as a function of time and displayed in Figure 5. It can be seen that there is an overall increase in the strength of the extrudate with mixing time irrespective of acid concentration.

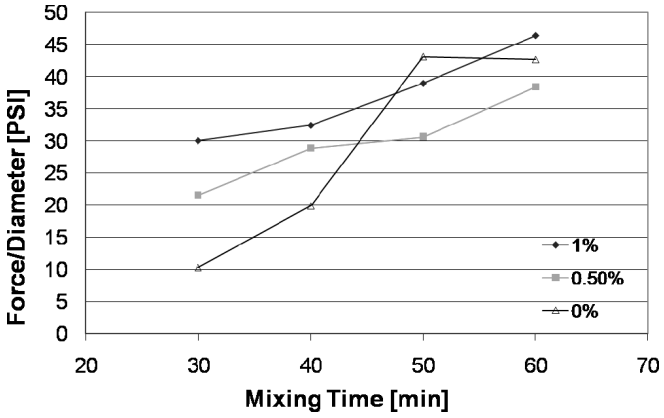

Fig. 5: Crush strength as a function of mixing time.

3.2 Paste Characterization

The properties of the paste will ultimately decide the characteristics of the calcined extrudate. One property that plays a significant role in the pore size distribution will be the particle size. Upon calcination the water present in the extrudates will begin to evaporate. This induces the particles to form inter particle bridges via neck formation thereby creating a pore network [12]. It can be seen from Figures 6 and 7 that as granulation time increases, there is a decrease in the overall particle size despite acid concentration. This shift to smaller particle sizes is coupled with a broadening effect in the particle size distribution.

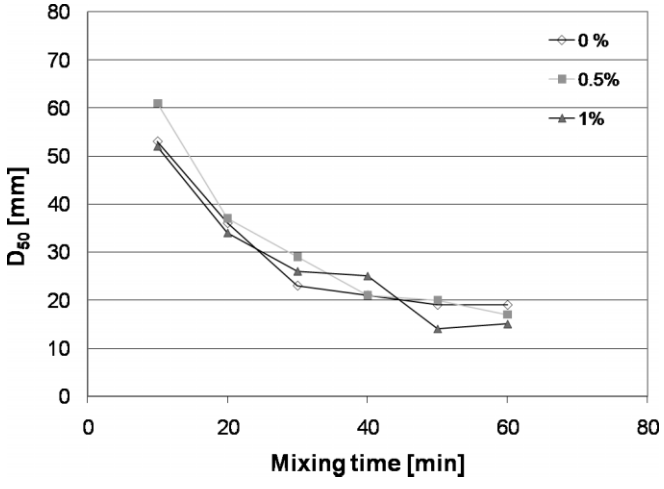

Fig. 6: D_{50} particle size values for the granulated samples as a function of mixing time for 0 %, 0.5 % and 1 % acid case.

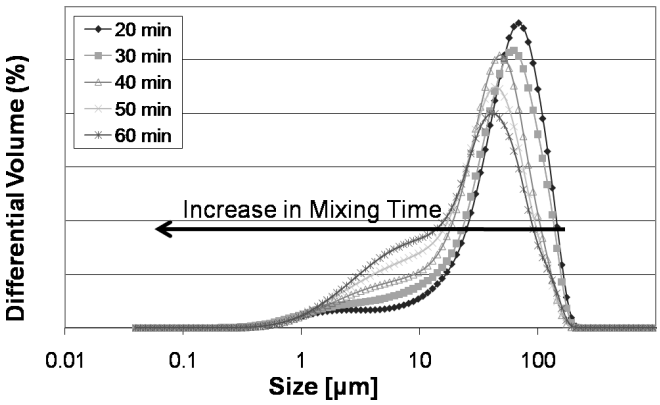

Fig. 7: Particle size distribution as a function of time for 1 % acid.

3.3 Comparative Investigation of Extrudates of Different Mixers

The bimodal distribution is thought to be the result of a higher severity inherent to the Fukae mixer. To verify this samples were produced in an Eirich mixer, a larger but less severe mixer whose (larger) blades operate at a sustained rate of 68 rpm, and is generally used in plant and pilot plant operations. At the conclusion of the mixing process, the batch was extruded with both a 2.25 inch single screw extruder (The Bonnet Company) and the 1/16th" die. This provided data through two avenues. First it allowed for the resultant pastes to be characterized by their respective particle size distribution. Second, by extruding the raw pastes with both the Bonnot extruder and the Carver press, two different extrusion techniques could be compared via N_2 porosimetry. These results are summarized in Figure 8 and Table 1. The particle size distributions are shown in Figure 6.

Unlike the Fukae mixer, which produces a bimodal pore size distribution, the Eirich mixer shows only one peak. The difference between the two is further reflected in the particle size distribution seen in Figure 9 for pastes mixed with the Eirich mixer which show an almost identical distribution with granulation time. But the overall properties- SA and PV- while higher for the more severe mixer, are not that dramatically different.

In addition, the crush strengths were measured to evaluate the extrudates resistance to fracture. These results show that it takes on average a force of 28.3 PSI to fracture the extrudates prepared by the Fukae mixer. This is compared to the 15.3 PSI that it takes to fracture those prepared by the Eirich mixer.

To date there has not been a report of a bimodal mesoporous size distribution using alumina without the need

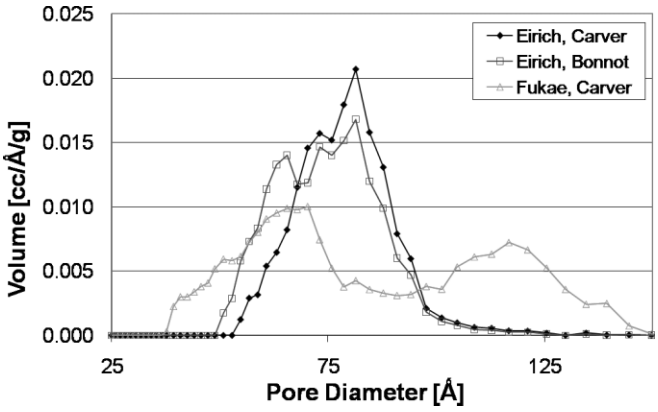

Fig. 8: Pore size distribution for pastes mixed and extruded by two different methods. The first term in parentheses signifies the type of mixer used, while the second term signifies the type of extruder used.

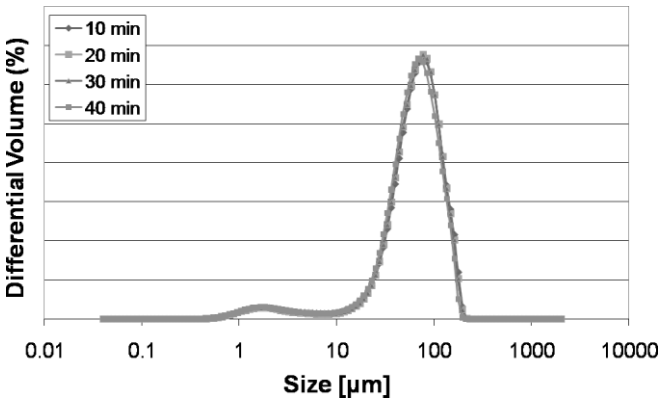

Fig. 9: Particle size distribution as a function of time for pastes prepared via Eirich mixer.

of a multi component alumina mixture. In order to see if the bimodal distribution that is presented here is inherent to the granules or manifests itself in the extrusion process, nitrogen porosimetry analysis was performed on the pre extruded pastes. Although not shown, these results demonstrate that there is a slight downshift to smaller pore sizes after extrusion, with the bimodal distribution still persisting. This is to be expected because the force required to extrude will in the process break down particles [14]. It can thus be determined that the bimodal distribution, although slightly affected by extrusion, is inherent to the granulation process itself.

4 Conclusion

It was revealed that a bimodal pore distribution develops as a function of alumina granulation time in a more severe mixer. Severity increases as a function of both higher blade speed and size. This higher severity is thought to be due to the high speed chopper present in the Fukae mixer, which ran at 1500 rpm in our experiments. This was tested against the apparently less severe Eirich mixer which showed only one peak in the pore size distribution. The values of pore size and pore volumes obtained in this study were found to be higher for the most part than those found in the synthesis of boehmite sol-gels [31]. The higher severity mixer produces a greater concentration of smaller particle sizes, which contributes to the formation of the bimodal pore size distribution at higher mixing times. Implementation of higher severity in larger scale mixers, perhaps by use of higher speed and larger choppers than now in use, could produce these bimodal distributions within the mesoporous range, if indeed that distribution actually produces improved catalysts.

Table 1: Summary of the surface area and pore volume for pastes prepared under different instrumental conditions. Results show the 0 % acid case mixed up to 40 minutes.

Solids: Binder (45 : 55) 0 % Acid	**Granulated: Fukae mixer Extruded: Carver press**	**Granulated: Eirich mixer Extruded: Carver press**	**Granulated: Eirich mixer Extruded: Bonnot extruder**
Multipoint Specific Surface Area (m^2/g)	304	260	289
Total Pore Volume at Po (0.990–0.998) (cm^3/g)	0.56	0.49	0.50
Single Point Specific Surface Area (m^2/g)	300	254	282
Average Pore Diameter (Å)	73*	76	0

* denotes the fact that the value is not truly representative of the average pore diameter but the average of the two peaks.

5 Acknowledgements

This work was supported in part by the Rutgers Catalyst Manufacturing Science and Engineering Consortium. AVN thanks Quantachrome Instruments for a free loan of adsorption equipment. AWC thanks M. S. Tomassone and J. Li for their help on the earlier stage of this project.

6 References

[1] M. E. Davis, Ordered porous materials for emerging applications. *Nature* **2002**, *417*, 813–821.

[2] S. H. Joo, S. J. Choi, I. Oh, J. Kwak, Z. Liu, O. Terasaki, R. Ryoo, Ordered nanoporous arrays of carbon supporting high dispersions of platinum nanoparticles. *Nature* **2001**, *412*, 169.

[3] C. T. Kresge, M. E. Leonowicz, W. J. Roth, J. C. Vartuli, J. S. Beck, Ordered mesoporous molecular sieves synthesized by a liquid-crystal template mechanism. *Nature* **1992**, *359*, 710 – 712.

[4] P. I. Ravikovitch, D. Wei, W. T. Chueh, G. L. Haller, A. V. Neimark, Evaluation of Pore Structure Parameters of MCM-41 Catalyst Supports and Catalysts by Means of Nitrogen and Argon Adsorption. *J. Phys. Chem. B* **1997**, *101*, 3671 – 3679.

[5] A. Sayari, Catalysis by Crystalline Mesoporous Molecular Sieves. *Chem. Mat.* **1996**, *8*, 1840 – 1852.

[6] A. Sayari, Nanoporous Materials IV. *Proc. of the 4th intern. symp. nanoporous materials Niagara Falls, Ontario, Canada*, June 7–10 2005, Gulf Professional Publishing, Amsterdam, **2005**.

[7] F. Q. Zhang, Y. Yan, Y. Meng, Y. Xia, B. Tu, D. Y. Zhao, Ordered bimodal mesoporous silica with tunable pore structure und morphology. *Microporous Mesoporous Mat.* **2007**, *98*, 6 – 15.

[8] Y. Zhang, M. Koike, N. Tsubaki, Multiple-Functional Capsule Catalyst: A Taylor-Made Confined Reaction. *Catal. Lett.* **2005**, *99*, 193 – 198.

[9] O. Levenspiel, *Chemical reaction engineering*, Wiley, New York, **1999**.

[10] S. Ananthakumar, P. Manohar, K. G. K. Warrier, Effect of boehmite and organic binder on extrusion of alumina. *Ceram. Int.* **2004**, *30*, 837 – 842.

[11] S. M. Iveson, J. D. Litster, K. Hapgood, B. J. Ennis, Nucleation, growth and breakage phenomena in agitated wet granulation processes: a review. *Powder Technol.* **2001**, *117*, 3 – 39.

[12] G. I. Tardos, M. I. Khan, P. R. Mort, Critical parameters and limiting conditions in binder granulation of fine powders. *Powder Technol.* **1997**, *94*, 245 – 258.

[13] J. J. Benbow, S. Blackburn, H. Mills, The effect of liquid-phase rheology on the extrusion behavior of paste. *J. Mater. Sci.* **1998**, *33*, 5827 – 5833.

[14] J. J. Benbow, J. Bridgewater, *Paste Flow and Extrusion*, Oxford, New York, **1993**.

[15] P. M. Eggerstedt, J. F. Zievers, E. C. Zievers, Choose the right ceramic for filtering hot gases. *Chem. Eng. Prog.* **1993**, *89 (1)*, 62 – 68.

[16] J. Cejka, Organized mesoporous alumina: synthesis, structure and potential in catalysis. *Appl. Catal. A-Gen.* **2003**, *254*, 327 – 338.

[17] C. Lesaint, G. Kleppa, D. Arla, W. R. Glomm, G. Oye, Synthesis and characterization of mesoporous alumina materials with large pore size prepared by a double hydrolysis route. *Microporous Mesoporous Mat.* **2009**, *119*, 245 – 251.

[18] D. L. Trimm, A. Stanislaus, The design of industrial catalysts. *Applied Catalysis* **1986**, *21*, 215.

[19] S. A. Bagshaw, T. J. Pinnavaia, Mesoporous alumina molecular sieves. *Angew. Chem.-Int. Edit. Engl.* **1996**, *35 (10)*, 1102 – 1105.

[20] S. Cabrera, J. El Haskouri, J. Alamo, A. Beltran, D. Beltran, S. Mendioroz, M. D. Marcos, P. Amoros, Surfactant-assisted synthesis of mesoporous alumina showing continuously adjustable pore sizes. *Adv. Mater.* **1999**, *11 (5)*, 379 – 381.

[21] F. Jiao, A. H. Hill, A. Harrison, A. Berko, A. V. Chadwick, P. G. Bruce, Synthesis of Ordered Mesoporous NiO with Crystalline Walls and a Bimodal Pore Size Distribution. *J. Am. Chem. Soc.* **2008**, *130*, 5262 – 5266.

[22] M. Kuemmel, D. Grosso, U. Boissiere, B. Smarsly, T. Brezesinski, P. A. Albouy, H. Amenitsch, C. Sanchez, Thermally stable nanocrystalline gamma-alumina layers with highly ordered 3D mesoporosity. *Angew. Chem.-Int. Edit.* **2005**, *44 (29)*, 4589 – 4592.

[23] K. Niesz, P. D. Yang, G. A. Somorjai, Sol-gel synthesis of ordered mesoporous alumina. *Chem. Commun.* **2005**, *15*, 1986 – 1987.

[24] B. Z. Tian, X. Y. Liu, B. Tu, C. Z. Yu, J. Fan, L. M. Wang, S. H. Xie, G. D. Stucky, D. Y. Zhao, Self-adjusted synthesis of ordered stable mesoporous minerals by acid-base pairs. *Nat. Mater.* **2003**, *2*, 159 – 163.

[25] Y. Zhang, X. Shi, J. M. Kim, D. Wu, Y. Sun, S. Y. Peng, Synthesis and catalysis of nanometer-sized bimodal mesoporous aluminosilicate materials. *Catal. Today* **2004**, *93 (5)*, 615 – 618.

[26] A. V. Neimark, P. I. Ravikovitch, Capillary condensation in MMS and pore structure characterization. *Microporous Mesoporous Mat.* **2001**, *44*, 697 – 707.

[27] P. I. Ravikovitch, G. L. Haller, A. V. Neimark, Density functional theory model for calculation pore size distributions: pore structure of nanoporous catalysts. *Adv. Colloid Interface Sci.* **1998**, *77*, 203 – 226.

[28] P. Holm, T. Schaefer, H. G. Kristensen, Granulation in high-speed mixers Part V. Power consumption and temperature changes during granulation. *Powder Technol.* **1985**, *43*, 213 – 223.

[29] K. Terashita, S. Watano, K. Miyanami, Determination of End-Point by Frequency Analysis of Power Consumption in Agitation Granulation. *Chem. Pharm. Bull.* **1990**, *38*, 3120 – 3123.

[30] Y. D. Li, D. F. Wu, J. P. Zhang, L. Chang, D. H. Wu, Z. P. Fang, Y. H. Shi, Measurement and statistics of single pellet mechanical strength of differently shaped catalysts. *Powder Technol.* **2000**, *113*, 176 – 184.

[31] Y. D. Li, X. M. Li, L. Chang, D. H. Wu, Z. P. Fang, Y. H. Shi, Understandings on the scattering property of the mechanical strength data of solid catalysts: A statistical analysis of iron-based high-temperature water-gas shift catalysts. *Catal. Today* **1999**, *51*, 73 – 84.

